Available online at www.sciencedirect.com
SCIENCE DIRECT
Biochemical Pharmacology 70 (2005) 1253–1261
Biochemical Pharmacology
www.elsevier.com/locate/biochempharm

The role of phenylalanine 483 in cytochrome P450 2D6 is strongly substrate dependent

Barbara M.A. Lussenburg [a], Peter H.J. Keizers [a], Chris de Graaf [a], Mats Hidestrand [b], M. Ingelman-Sundberg [b], Nico P.E. Vermeulen [a], Jan N.M. Commandeur [a,*]

[a] *LACDR/Division of Molecular Toxicology, Department of Pharmacochemistry, Vrije Universiteit, De Boelelaan 1083, 1081 HV Amsterdam, The Netherlands*

[b] *Division of Molecular Toxicology, Institute of Environmental Medicine, Karolinska Institutet, 171 77 Stockholm, Sweden*

Received 9 May 2005; accepted 1 July 2005

Abstract

The polymorphic cytochrome P450 2D6 (CYP2D6) is involved in the metabolism of 30% of the drugs currently prescribed, and is thus clinically relevant. Typical CYP2D6 substrates generally contain a basic nitrogen atom and an aromatic moiety adjacent to the site of metabolism. Recently, we demonstrated the importance of active site residue F120 in substrate binding and catalysis in CYP2D6. On the basis of protein homology models, it is claimed that another active site phenylalanine, F483, may also play an important role in the interaction with the aromatic moiety of CYP2D6 substrates. Experimental data to support this hypothesis, however, is not yet available. In fact, in the only study performed, mutation of F483 to isoleucine or tryptophan did not affect the 1′-hydroxylation of bufuralol at all [Smith G, Modi S, Pillai I, Lian LY, Sutcliffe MJ, Pritchard MP, et al., Determinants of the substrate specificity of human cytochrome P-450 CYP2D6: design and construction of a mutant with testosterone hydroxylase activity. Biochem J 1998;331:783–92]. In the present study, the role of F483 in ligand binding and metabolism by CYP2D6 was examined experimentally using site-directed mutagenesis. Replacement of F483 by alanine resulted in a 30-fold lower V_{max} for bufuralol 1′-hydroxylation, while the K_m was hardly affected. The V_{max} for 3,4-methylenedioxy-methylamphetamine *O*-demethylenation on the other hand decreased only two-fold, whereas the effect on the K_m was much larger. For dextromethorphan, in addition to dextrorphan (*O*-demethylation) and 3-methoxymorphinan (*N*-demethylation), two other metabolites were formed that could not be detected for the wild-type. The substrate 7-methoxy-4-(aminomethyl)-coumarin was not metabolised at all by CYP2D6[F483A], a phenomenon that was reported also for CYP2D6[F120A]. The presented data show that next to F120, residue F483 plays a very important role in the metabolism of typical CYP2D6 substrates. The influence of F483 on metabolism was found to be strongly substrate-dependent.

Keywords: Cytochrome P450 2D6; Active site; Site-directed mutagenesis; Phenylalanine 483; Substrate selectivity

1. Introduction

The cytochrome P450 superfamily constitutes a large group of oxido-reductases that are responsible for the oxidation and reduction of many endogenous compounds as well as a wide variety of xenobiotics [1–3]. In humans, cytochrome P450 2D6 (CYP2D6) is one of the most important enzymes of this family [4]. Despite its low abundance – CYP2D6 represents only 4–8% of the total cytochrome P450 in human liver – it metabolises ~30% of the drugs currently on the market [5,6]. Its clinical relevance is even increased by the fact that CYP2D6 is highly polymorphic; 6% of the European population is classified as a 'poor metaboliser', while another 3% has the 'ultra-rapid metaboliser' phenotype [6–9], thus contributing to large interindividual differences in drug metabolism.

The development of accurate models of the active site of CYP2D6 is very useful to identify potential drug candidates that interact with the enzyme. Because no crystal structure is

Abbreviations: CYP, cytochrome P450; CPR, cytochrome P450 reductase; FU, fluorescence units; HAMC, 7-hydroxy-4-(aminomethyl)-coumarin; MAMC, 7-methoxy-4-(aminomethyl)-coumarin; MDMA, 3,4-methylenedioxy-methylamphetamine; MDA, 3,4-methylenedioxy-amphetamine; 3,4-OH-MA, 3,4-dihydroxy-methylamphetamine

* Corresponding author. Tel.: +31 20 5987595; fax: +31 20 5987610.
E-mail address: jnm.commandeur@few.vu.nl (Jan N.M. Commandeur).

0006-2952/$ – see front matter © 2005 Elsevier Inc. All rights reserved.
doi:10.1016/j.bcp.2005.07.002

yet available for CYP2D6, the structural information required for such models has to be obtained from homology modeling [10,11] and experimental mutagenesis studies.

Most substrates of CYP2D6 contain a basic nitrogen at a distance of approximately 5–7 Å from the site of oxidation, and an adjacent aromatic moiety [12]. The negatively charged active site residues E216 and D301 have been shown to play a role in fixation of the basic nitrogen atom [13–15]. Pharmacophore and homology models suggest a role for aromatic residues in the active site to undergo VanderWaals interactions with aromatic moieties of the ligands [16]. Three aromatic phenylalanine residues have been proposed as active-site residues, F120, F481 and F483. Recently, it was experimentally underlined that F120 is indeed one of the aromatic active site residues that plays an important role in substrate binding and metabolism [17,18]. In earlier CYP2D6 homology models based on bacterial cytochrome P450 crystal structure templates it was suggested that another aromatic residue associated with ligand binding is F481 [16,19,20]. Substitution of F481 by non-aromatic residues reduced the affinity of several typical CYP2D6 substrates [16]. In more recent homology models based on rabbit CYP2C5, however, F481 is positioned outside the binding pocket, but in close contact with active site residue F483 [14,21–23]. Our model (Fig. 1) [21] and several others [14,22–24] suggest that this aromatic active site residue, i.e. F483, is also a potential ligand-contact residue (Fig. 1). In a modeling study by Kemp et al. phenylalanines 120 and 483 are referred to as very important residues in the active site of CYP2D6, which are involved in the binding of various NCI compounds [24]. However, experimental data supporting a role for F483 in binding known CYP2D6 substrates is not yet available. In fact, in the only experimental study on this residue, it was shown that substitution of F483 by isoleucine or tryptophan did not affect the 1′-hydroxylation of the typical CYP2D6 substrate bufuralol [23]. Interestingly, the F483I mutant was able to catalyse the 15α-hydroxylation of testosterone, which is not a substrate for wild-type CYP2D6 [23]. Therefore, it is not yet clear whether this residue plays a role in the binding of typical CYP2D6 substrates. Recently, we demonstrated that the role of another active-site phenylalanine-residue, F120, is very substrate dependent [17,18]. The F120A mutant completely lost the ability to metabolise 7-methoxy-4-(aminomethyl)coumarin

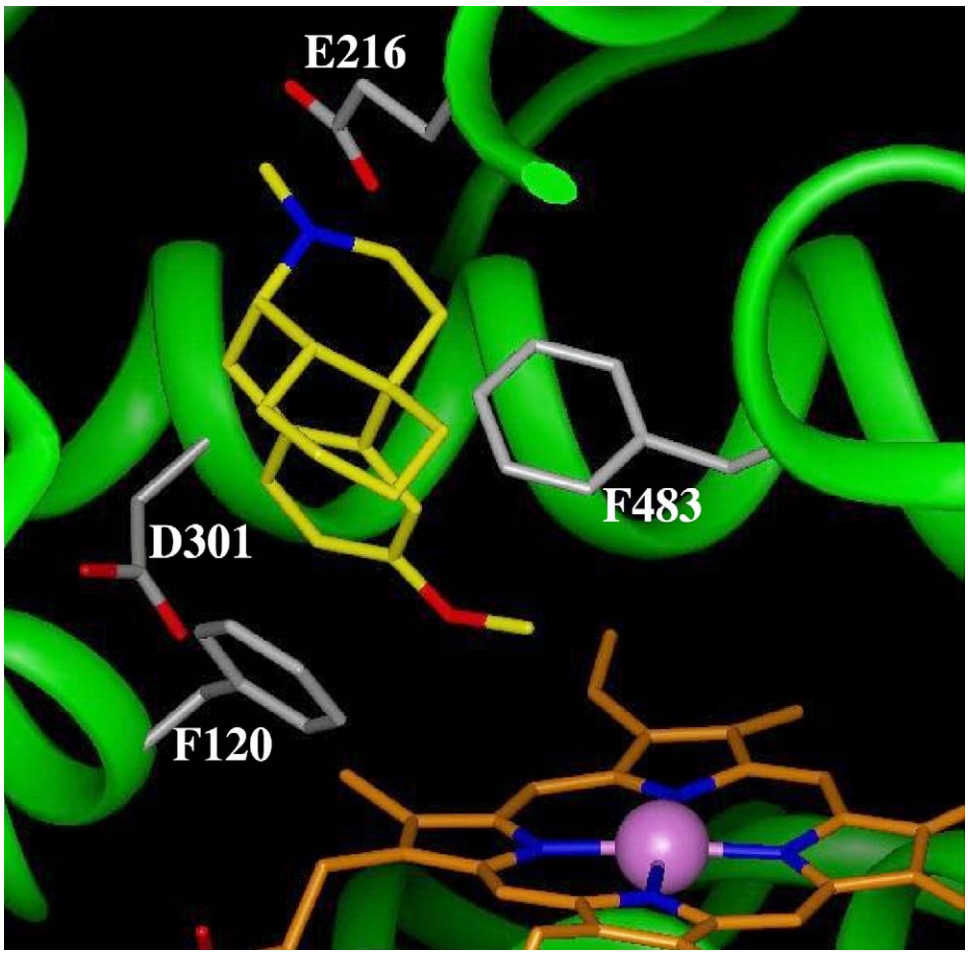

Fig. 1. The active site of the homology model of CYP2D6 [17], showing the active site residues F120, E216, D301 and F483. The pink ball at the bottom represents the heme iron atom. In yellow, the substrate dextromethorphan is depicted. (For interpretation of the references to color in this figure legend, the reader is referred to the web version of this article.)

(MAMC), while no significant effect on bufuralol metabolism was observed. 3,4-Methylenedioxymethamphetamine (MDMA) and dextromethorphan were still metabolised by F120A, but the regiospecificity of metabolism had changed significantly.

The goal of the present study is to investigate whether the role of phenylalanine F483 in the metabolism of typical CYP2D6 substrates is substrate dependent. Using site-directed mutagenesis, this phenylalanine residue was substituted by an alanine (F483A), and the effect of this mutation on the binding and metabolism of four typical CYP2D6 substrates, notably dextromethorphan, bufuralol, MDMA and MAMC, was studied.

2. Materials and methods

2.1. Materials

7-Methoxy-4-(aminomethyl)-coumarin (MAMC), 7-hydroxy-4-(aminomethyl)-coumarin (HAMC), 3,4-methylenedioxymethylamphetamine (MDMA) and 3,4-methylenedioxyamphetamine (MDA) were synthesised as described [25,26]. Bufuralol hydrochloride was obtained from Gentest. *N*-Methylhydroxylamine hydrochloride, dextromethorphan hydrobromide and dextrorphan tartrate were obtained from Sigma. All other chemicals were of analytical grade and obtained from standard suppliers.

2.2. Plasmid and site-directed mutagenesis

The pSP19T7LT_2D6 plasmid containing human CYP2D6 with a C-terminal His_6-tag bicistronically co-expressed with human Cytochrome P450 NADPH reductase (CPR) was constructed as follows: the CPR was generated by reverse transcription of human genomic DNA using a reverse transcription kit with oligo dT primers (Clontech Inc., USA). After reverse transcription, the cDNA was amplified with primers creating restriction enzyme cut sites. Human CYP2D6 was amplified from a cDNA. During amplification additional C-terminal histidines as well as sites for restriction enzyme cleavage were introduced. The amplified and digested 2D6 and CPR were subsequently ligated into the expression plasmid pSP19T7LT [27] in tandem, with a short linker region in-between the two genes. The correct gene sequence was verified by sequencing.

The phenylalanine 483 to alanine (F483A) mutation was introduced into pSP19T7LT_2D6 using the QuikChange XL Site-Directed Mutagenesis kit (Stratagene). The sequences of the forward- and reverse oligonucleotides, respectively, with the altered nucleotides in italic, were as follows: 5′-AT-GGT-GTC-TTT-GCT-*GCC*-CTG-GTG-AGC-CC-3′ and 5′-GG-GCT-CAC-CAG-*GGC*-AGC-AAA-GAC-ACC-AT-3′. After mutagenesis, the presence of the desired F483A mutation was confirmed by DNA sequencing.

2.3. Expression and membrane isolation

The plasmids pSP19T7LT_2D6 and pSP19T7LT_2D6-[F483A] were transformed into *Escherichia coli* strain JM109. Expression was carried out in 3 l flasks containing 300 ml TB (Terrific Broth) medium with additives (1 mM δ-aminolevulinic acid, 400 μl/l trace elements [28], 1 μg/ml thiamine, 100 μg/ml ampicillin). Cultures were inoculated with 3 ml frozen *E. coli* cells containing the desired plasmid, and expression of CYP2D6 and CPR was initiated by the addition of 2 mM isopropyl-β-D-thiogalactopyranoside (IPTG). Cultures were grown for 48 h at 28 °C and 125 rpm, before they were harvested. CYP contents were determined by carbon monooxide (CO) difference spectra [29].

Harvested cells were pelleted by centrifugation (15 min, 4000 × *g*, 4 °C) and the resulting pellet was resuspended in 1/20 original culture volume of Tris-Sucrose-EDTA (TSE) buffer (50 mM Tris–acetate, pH 7.6, 250 mM sucrose, 0.25 mM EDTA). After the addition of 0.1 mg/ml lysozyme, the cells were disrupted using a French Press (1000 psi, three repeats). To remove remaining undisrupted cells, the lysate was centrifuged (15 min, 4000 × *g*, 4 °C) and the resulting pellet was discarded. The cytosolic fraction was separated from the membranous fraction by ultracentrifugation in a Beckmann 50.2Ti rotor (45 min, 120,000 × *g*, 4 °C). The membrane pellet was resuspended in 1/75 original culture volume of TSE buffer and CYP contents were determined using CO difference spectra. CPR activity was measured using cytochrome c reduction as described previously [30,31]. The CPR concentrations were calculated from the CPR activities based on a specific activity of 3200 nmol cytochrome C/min/nmol reductase, as described previously [30,31].

For determination of dissociation constants of ligands, the CYP was purified from the membranes. Enzymes were solubilised by stirring for 2 h at 4 °C in KPi-glycerol buffer (50 mM potassium phosphate buffer pH 7.4 with 10% glycerol), supplemented with 0.5% Emulgen 911. Insoluble parts were removed by centrifugation (60 min, 120,000 × *g*, 4 °C). Supernatant was incubated, gently rocking, with Ni-NTA agarose for 30 min at 4 °C. The column material was retained in a polypropylene tube with porous disc (Pierce), washed with KPi-glycerol buffer containing 2 mM histidine. CYP2D6 was eluted with 0.2 M histidine. After overnight dialysis in KPi-glycerol buffer the sample was concentrated on a Vivaspin 20 filtration tube (10,000 MWCO PES, Sartorius).

2.4. Metabolism of model compounds

Before the enzyme kinetic parameters of the four substrates were determined, a series of experiments was performed to determine the linearity of the reactions with time and enzyme concentration. Based on these

experiments (data not shown), incubation times and enzyme concentrations were chosen that are within the linear range.

2.4.1. MAMC metabolism [25,32]

Reactions were carried out in triplicate in a black Costar 96-well plates, in a total volume of 200 μl. The reaction mixture consisted of 100 mM potassium phosphate buffer (KPi) pH 7.4 with 5 mM $MgCl_2$ and 2 mM EDTA, and *E. coli* membranes containing 40 nM CYP2D6 (wild-type or CYP2D6[F483A]) and CPR. Nine different concentrations of MAMC were used ranging from 0 to 320 μM. The reaction was initiated by addition of an NADPH regenerating system, resulting in final concentrations of 0.1 mM NADPH, 0.3 mM glucose-6-phosphate and 0.4 units/ml glucose-6-phosphate dehydrogenase. The reaction was monitored for 30 min at 37 °C on a Victor^2 1420 multilabel counter (Wallac) (λ_{ex} = 405 nm, λ_{em} = 460 nm). The metabolite of MAMC, i.e. HAMC, was identified and quantified using the synthetic reference compound. Samples were also analysed by high-performance liquid chromatography (HPLC) as described previously [25] to determine if other metabolites were formed that could not be detected on the fluorescence microplate reader.

2.4.2. Dextromethorphan metabolism [15]

The reaction mixture was composed as described for MAMC, with *E. coli* membranes containing 25 nM CYP2D6 (wild-type or CYP2D6[F483A]) and CPR. Ten different concentrations of dextromethorphan were used ranging from 0 to 80 μM. After 5 min of preincubation at 37 °C, the reaction was initiated by addition of an NADPH regenerating system as described above. The reaction was allowed to take place for 10 min at 37 °C before it was stopped with 1/20 volume of 70% $HClO_4$. Precipitated proteins were removed by centrifugation (10 min, 6800 × *g*), and the supernatant was analysed by HPLC (injection volume 25 μl). Metabolites were separated using a C18 column (Phenomenex Luna 5 μm, 150 mm × 4.6 mm) with a flow rate of 0.6 ml/min. The mobile phase consisted of 30% acetonitril (ACN) and 0.1% triethylamine, set to pH 3 with $HClO_4$. Metabolites were detected by fluorescence (λ_{ex} = 280 nm, λ_{em} = 311 nm). The metabolite dextrorphan was identified using co-elution with the reference compound; other metabolites were identified by liquid chromatography–mass spectrometry (LC–MS).

2.4.3. Bufuralol metabolism [15,33]

Reactions were carried out as described above for dextromethorphan, with nine concentrations of bufuralol ranging from 0 to 80 μM. Metabolites were separated using a C18 column (Phenomenex Luna 5 μm, 150 mm × 4.6 mm) with a flow rate of 0.6 ml/min. The mobile phase consisted of 30% ACN and 0.1% triethylamine, set to pH 3 with $HClO_4$. Metabolites were detected by fluorescence (λ_{ex} = 252 nm, λ_{em} = 302 nm). Metabolites of bufuralol were identified by comparing retention times and relative peak areas with those described in previous studies [33]; 1′-OH bufuralol was identified using co-elution with a reference compound. LC/MS was used to identify $\Delta^{1,2}$-bufuralol (data not shown).

2.4.4. MDMA metabolism [34]

Reactions were carried out as described above with nine concentrations of MDMA ranging from 0 to 220 μM. Metabolites were separated using a C18 column (Phenomenex Luna 5 μm, 150 mm × 4.6 mm) with a flow rate of 0.6 ml/min. The mobile phase consisted of 22% ACN and 0.1% triethylamine, set to pH 3 with $HClO_4$. Metabolites were detected by fluorescence (λ_{ex} = 280 nm, λ_{em} = 320 nm). MDA was identified using the synthesised reference compound, and the catechol 3,4-dihydroxy-methylamphetamine (3,4-OH-MA) was identified previously using electrochemical detection [17].

Peak areas of all metabolites were quantified by the Shimadzu Class VP 4.3 software package. Reaction rates were calculated and plotted against the substrate concentrations to obtain Michaelis Menten curves, and the 'one site binding hyperbola fitting' module of Graph Pad Prism 4.0 was used to estimate K_m and V_{max} values.

2.5. Identification of metabolites using LC–MS

To identify the unknown metabolites of dextromethorphan, LC–MS was used. For LC–MS measurements, incubations were carried out as described above with 40 μM dextromethorphan, and *E. coli* membranes containing 25 nM CYP2D6 (wild-type or CYP2D6[F483A]), and CPR. Volumes of 50 μl supernatant were injected and separated using a phenyl column (Phenomenex Phenyl 150 mm × 4.6 mm) with a flow rate of 0.6 ml/min. The metabolites were eluted using a gradient starting with a 5% ACN eluens, supplemented with 20 mM ammonium acetate, increasing linearly to 90% ACN with 20 mM ammoniumacetate in 14 min and analysed by MS. Positive ion Atmospheric Pressure Chemical Ionisation (APCI) was used on a LCQ Deca mass spectrometer (Thermo Finnigan), vaporizer temperature 450 °C, N_2 as sheath (40 psi) and as auxiliary gas (10 psi), needle voltage 6000 V, heated capillary 150 °C. MS/MS was performed with an activation energy of 30%.

2.6. Determination of dissociation constants

Dissociation constants were determined for dextromethorphan, bufuralol and MDMA in disposable 1 ml cuvettes. Two cuvettes were prepared containing 1 μM of purified CYP (wild-type or CYP2D6[F483A]) in a final volume of 500 μl 100 mM potassium phosphate buffer (KPi) pH 7.4. Aliquots of 5 μl of a 1 mM ligand solution in KPi buffer were added to the sample cuvette, while the

same amount of KPi buffer was added to the reference cuvette. Difference spectra from 350 to 450 nm were taken after every addition. In total, 11 aliquots were added, which corresponds to a ligand concentration ranging from 10 μM (addition 1) to 104 μM (addition 11). Upon type 1 binding of the substrates, a peak at 390 nm and a trough at 420 nm appeared. The ΔAbs (390–420 nm) values were plotted against the ligand concentration, and the 'one site binding hyperbola fitting' module of Graph Pad Prism 4.0 was used to estimate the dissociation constants (K_d).

3. Results

3.1. Expression of CYP2D6 and CYP2D6[F483A]

CYP2D6 and CYP2D6[F483A] were successfully expressed in *E. coli*. A typical cell culture yielded approximately 400 nM CYP, and the expression levels of CYP (Fig. 2) were not affected by the presence of the F483A mutation. The CYP and CPR concentrations in the membranes were similar for wild-type CYP2D6 and CYP2D6[F483A], as summarized in Table 1. The purified fractions contained 50 ± 5 μM of CYP for wild-type and mutant. The CYP content of wild-type and mutant membranes or purified fractions did not decrease significantly after storage of up to six months at −80 °C and repeated cycles of freeze-thawing, indicating that the stability of the enzyme was not significantly influenced by the mutation.

A substantial amount of P420, the inactive form of CYP, could also be detected in the whole cell fractions and in the membrane factions. The amount of P420 in wild-type CYP2D6 and CYP2D6[F483A] was similar (Fig. 2). In the purified fractions, no P420 could be detected.

3.2. Metabolism of model compounds

The CYP2D6 marker substrate MAMC was *O*-demethylated by wild-type CYP2D6 with a K_m of 42 μM and a V_{max} of 2.0 min^{-1} (Table 2). In contrast, the CYP2D6[F483A] mutant did not form any detectable

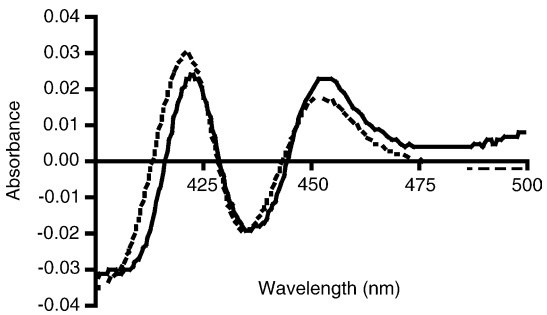

Fig. 2. CO-difference spectra of *E. coli* JM109 cells expressing CYP2D6 and CYP2D6[F483A]. The cell samples, taken after 48h of expression, were diluted two-fold before the spectra were recorded. Solid line: wild-type CYP2D6; dashed line: CYP2D6[F483A]. Both spectra correspond to approximately 200 nM CYP protein.

Table 1
CYP- and CPR concentrations in membrane fractions

	Wild-type	F483A
[CYP] membranes (μM)	8.1 ± 0.8	7.9 ± 0.7
[CPR] membranes (μM)	4.7 ± 0.5	4.0 ± 0.5
Ratio [CYP]/[CPR]	1.7 ± 0.3	2.0 ± 0.3

CPR concentrations were calculated from CPR activities of 15 mM Cyt C/min for CYP2D6 and 12.9 mM Cyt C/min for CYP2D6[F483A] by dividing by 3200 mM Cyt C/min/nmol CPR.

HAMC; re-analysis of the samples using HPLC also showed no detectable metabolites of MAMC.

The main metabolite formed upon dextromethorphan metabolism by wild-type CYP2D6 was the *O*-demethylated form, dextrorphan (Table 2) (*m/z* 258 and MS/MS *m/z* 201). In addition, trace amounts of the *N*-demethylated compound, 3-methoxymorphinan (*m/z* 258 and MS/MS *m/z* 215), were detected, but the amounts were too low to determine accurate enzyme kinetic parameters (Fig. 4). CYP2D6[F483A] also formed dextrorphan, with a 15-fold higher K_m and a two-fold higher V_{max} than the wild-type resulting in a 7.5-fold lower V_{max}/K_m. 3-Methoxymorphinan was formed by CYP2D6[F483A] with higher activity than wild-type CYP2D6, and V_{max} and K_m values could be determined (Table 2). In addition, trace amounts of two other metabolites were observed (Fig. 4). LC–MS analysis showed that these were the double (*O*- and *N*-)demethylated 3-hydroxymorphinan (*m/z* 244 and MS/MS *m/z* 201), and the monohydroxylated, *O*-demethylated hydroxydextrorphan (*m/z* 274 and MS/MS *m/z* 217), respectively.

Bufuralol was metabolised by wild-type CYP2D6 into three detectable metabolites, 1′-OH-bufuralol, 4-OH-bufuralol and $\Delta^{1',2'}$-bufuralol, as described before [17] (Table 2). Although the K_m values of CYP2D6 and CYP2D6[F483A] for bufuralol 1′-hydroxylation were very similar, the V_{max} of CYP2D6[F483A] was 32-fold lower. Under the conditions applied, only 1′-OH-bufuralol and trace amounts of 4-OH-bufuralol could be detected for CYP2D6[F483A] (Table 2).

MDMA was converted by wild-type CYP2D6 mainly to the catechol 3,4-OH-MA with a K_m of 2.2 μM and a V_{max} of 1.7×10^5 fluorescence units/(min nmol) CYP. Only trace amounts of MDA [34] were detected. CYP2D6[F483A] formed 3,4-OH-MA with a 13-fold higher K_m and a 2-fold lower V_{max}, resulting in a 26-fold lower V_{max}/K_m value (Table 2). Like for wild-type CYP2D6, trace amounts of MDA were also observed for CYP2D6[F483A]. In contrast to the F120A mutant, no detectable *N*-hydroxylation of MDMA was performed by CYP2D6[F483A] [17].

3.3. Determination of dissociation constants

The K_d values of dextromethorphan, bufuralol and MDMA were determined for wild-type CYP2D6 and for CYP2D6[F483A] (Table 3). For MAMC, no K_d values

Table 2
Kinetic parameters of wild-type CYP2D6 and CYP2D6[F483A] towards several typical CYP2D6 substrates

Compound	Metabolites	Wild-type			F483A		
		K_m	V_{max}	V_{max}/K_m	K_m	V_{max}	V_{max}/K_m
MAMC	HAMC	42.4 ± 2.6	2.0 ± 0.1[a]	0.050 ± 0.003	–[b]	–[b]	–
Dextromethorphan	Dextrorphan	1.1 ± 0.1	5.6 ± 0.1[a]	5.1 ± 0.4	17.0 ± 1.3	11.5 ± 0.3[a]	0.68 ± 0.06
	3-OMe-morphinan	+[c]	+[c]	–	64.9 ± 5.7	80.0 ± 4.0[d]	1.2 ± 0.1
	3-OH-Morphinan	–[b]	–[b]	–	+[c]	+[c]	–
	OH-Dextrorphan	–[b]	–[b]	–	+[c]	+[c]	–
Bufuralol	1′-OH-Bufuralol	5.0 ± 0.1	14.5 ± 2.0[d]	2.9 ± 0.4	4.6 ± 0.4	0.43 ± 0.01[d]	0.09 ± 0.01
	4-OH-Bufuralol	5.8 ± 0.1	1.3 ± 0.2[d]	0.2 ± 0.1	+[c]	+[c]	–
	$\Delta^{1',2'}$-Bufuralol	23.0 ± 5.4	1.3 ± 0.1[d]	0.06 ± 0.01	–[b]	–[b]	–
MDMA	3,4-OH-MA	2.2 ± 0.3	1.7 ± 0.1[d]	0.8 ± 0.5	28.6 ± 3.9	0.80 ± 0.03[d]	0.030 ± 0.004
	MDA	+[c]	+[c]	–	+[c]	+[c]	–

All values are the means of at least three independent experiments (performed on separate days) ±S.D. as described in the experimental section. K_m values are expressed in μM.
[a] V_{max} values expressed in min^{-1}.
[b] Not detectable.
[c] Present but not quantifiable.
[d] V_{max} values expressed in 1×10^5 fluorescence units/ (min nmol) P450.

could be determined because this ligand has a very high absorption at 350–450 nm that interfered with the binding spectra. Dextromethorphan, bufuralol and MDMA all showed type 1 spectra for CYP2D6 and CYP2D6[F483A], indicating that the ligands bind at the substrate binding site. No large differences were found between K_d values for CYP2D6 and CYP2D6[F483A]. K_d values of dextromethorphan and bufuralol were both in the range of 20–30 μM for wild-type CYP2D6 and CYP2D6[F483A], while the K_d values of MDMA were higher for both enzymes (50–60 μM).

4. Discussion

The aim of this study was to investigate the role of CYP2D6 active site residue F483 in ligand binding and metabolism. Aromatic residues in the CYP2D6 active site cavity are thought to be particularly important because of their ability to interact with aromatic moieties present in many CYP2D6 substrates [12]. Recently, it has been described that substitution of active site F120 by an alanine has large substrate dependent effects on the binding and metabolism of typical CYP2D6 substrates [17,18]. Homology modeling studies have also suggested an important role for residue F483 [14,21–24], but to date experimental evidence supporting this suggestion was not available. The results presented in this study clearly show that substitution of the phenylalanine moiety at position 483 by an alanine (F483A) has marked effects on substrate selectivity and regiospecificity when using four typical CYP2D6 substrates (Fig. 3). The observed effects of the F483A mutation were found to be strongly substrate-dependent, as was seen recently for F120A.

CYP2D6[F483A] did not metabolise MAMC, in contrast to wild-type CYP2D6. Apparently, residue F483 (this study) and residue F120 [17] are both required for metabolism of this substrate. These residues could either provide steric constraints to keep the substrate in the orientation required for metabolism, or they could function as aromatic anchoring points. A possible explanation is that MAMC is kept into position by both phenylalanines in a 'sandwich' configuration.

Table 3
Dissociation constants of ligands for CYP2D6 and CYP2D6[F483A]

Ligand	K_d (μM) wild-type		K_d (μM) F483A	
Dextromethorphan	23.9 ± 1.1	21.9 ± 0.7	29.5 ± 1.5	38.1 ± 3.5
Bufuralol	19.4 ± 2.0	15.4 ± 1.2	18.2 ± 1.4	21.8 ± 1.9
MDMA	34.5 ± 2.1	51.5 ± 3.6	52.4 ± 5.0	60.7 ± 7.1

Dissociation constants were determined in two separate experiments as described in Section 2. Each value represents an independent experiment. The 11 data points were analysed in Graphpad Prism using the 'one site binding hyperbola fitting' module. The standard errors of the fits are shown in the table.

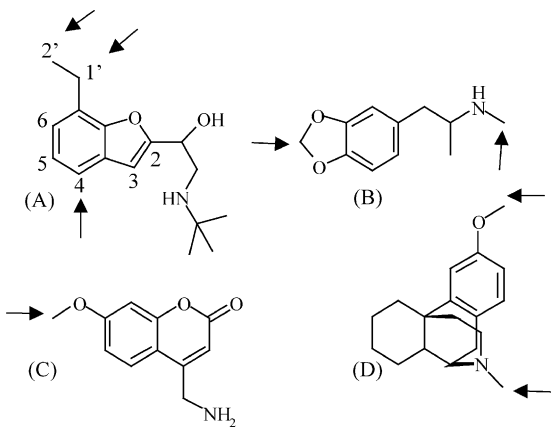

Fig. 3. Structures of four typical CYP2D6 substrates. (A) Bufuralol, (B) MDMA, (C) MAMC and (D) dextromethorphan. Sites of oxidation by wild-type CYP2D6 are indicated by arrows.

Dextromethorphan is believed to bind by electrostatic interactions between its basic nitrogen atom and the acidic residues E216 and D301 [15]. Recently, it has been shown that aromatic residue F120 also plays a role in dextromethorphan metabolism, since substitution of this residue resulted in the formation of two novel metabolites [17,18]. The present study shows that residue F483 is also involved in metabolism of dextromethorphan. Wild-type CYP2D6 performes mainly *O*-demethylation of dextromethorphan, while F483A also formed substantial amounts of *N*-demethylated product. In addition, two extra metabolites were formed (Fig. 4) that could not be detected in wild-type CYP2D6 incubations, but have been described previously for CYP2D6[F120A] [17,18]. The K_d values of dextromethorphan were similar for wild-type CYP2D6 and CYP2D6[F483A] (Table 3), indicating that the binding affinity of dextromethorphan is not greatly affected by the mutation. The observed effects on the metabolic ratio may therefore result from the different orientations that can be adopted by the large, non-flat substrate dextromethorphan in the active site of CYP2D6[F483A], as a consequence of the increased available space.

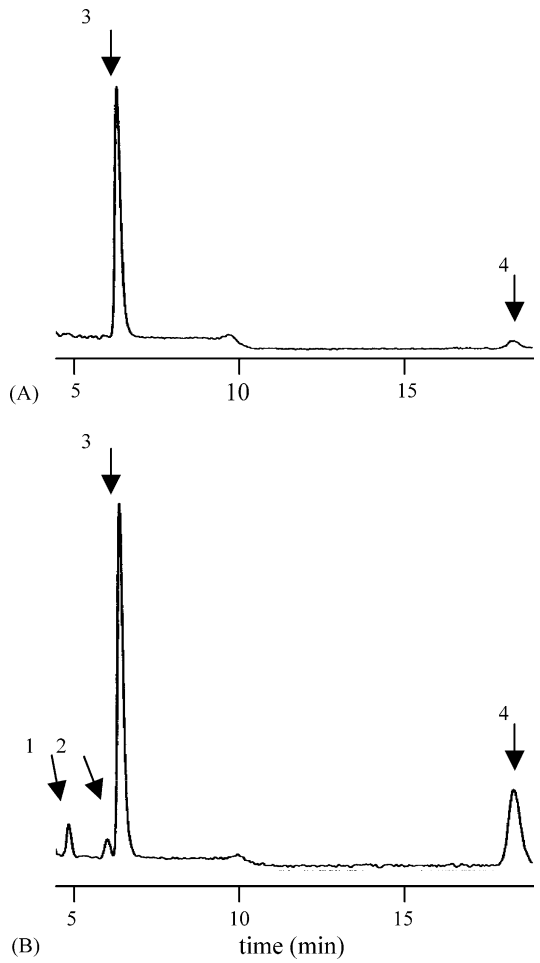

Fig. 4. HPLC chromatograms of dextromethorphan metabolism by wild-type CYP2D6 (A) or CYP2D6[F483A] (B). Incubations were carried out as described in the experimental section. Metabolites indicated by arrows are: (1) hydroxy-dextrorphan; (2) 3-hydroxymorphinan; (3) dextrorphan and (4) 3-methoxymorphinan. The substrate dextromethorphan has a retention time of 24 min and is not displayed in these chromatograms.

For bufuralol metabolism, the acidic residues E216 and D301 have been shown to be very important because they are involved in the fixation of the basic nitrogen of bufuralol [14,15,33]. Mutagenesis of aromatic residue F120 to alanine, on the other hand, did not significantly affect the metabolism of this substrate [17]. In a previous mutagenesis study, it was found that the substitution of F483 by tryptophan or isoleucine also had no influence on bufuralol 1′-hydroxylation [23]. In the present study, however, a significant effect on bufuralol metabolism was observed when F483 was replaced by the smaller alanine. This mutation resulted in a 32-fold lower V_{max} for bufuralol 1′-hydroxylation, while the K_m value was hardly affected. The binding affinity of bufuralol was not significantly influenced by the F483A mutation (Table 3). The fact that the more conservative substitutions of F483 by tryptophan and isoleucine have no effect on bufuralol metabolism suggests that these amino acid residues can compensate for the loss of the phenylalanine-residue, by aromatic, hydrophobic, and/or steric interaction with bufuralol.

Previous studies with CYP2D6[F120A] showed that for this mutant, regioselectivity of MDMA metabolism had changed significantly. The amount of MDA produced by this mutant was greatly increased compared to wild-type CYP2D6. In addition, a novel metabolite was formed which could be identified as *N*-OH-MDMA [17]. In the present study, it was shown that the effect of a F483A substitution on MDMA did not influence the metabolic ratio, but only affected the kinetic parameters of 3,4-OH-MA formation (Table 2). For the formation of the major metabolite 3,4-OH-MA, the K_m value of CYP2D6[F483A] was 13-fold higher than the wild-type value, while the V_{max} value decreased only two-fold (Table 2). The K_d value of MDMA was very similar for wild-type CYP2D6 and CYP2D6[F483A] (Table 3). The fact that the changes in K_m value and the K_d value do not follow the same trend may be explained by the fact that the K_m and K_d values actually represent qualitatively different processes. The K_d value, which is determined by difference spectroscopy, is describing the ability of a ligand to induce a spin shift of the heme-iron in absence of NADPH. The parameter K_m is related to the enzyme reaction and its value is determined by both binding affinity and rate limiting steps of the catalytic reaction [35].

Residue F120 was shown to be very important for MDMA metabolism, but not for bufuralol metabolism [17], while for F483A bufuralol metabolism and MDMA metabolism are both affected by the mutation. For bufuralol, only the V_{max} was altered, while for MDMA mainly the K_m was influenced by the mutation. These results suggest that these two compounds have different modes of binding, despite their high degree of structural similarity.

In conclusion, the data presented in this study prove that F483 plays an important role in CYP2D6 selectivity and activity. Together with acidic residues E216 and D301 and aromatic residue F120, it defines the ligand binding properties and the regiospecificity of metabolism. However, of the at least 25 residues postulated to form the active site of CYP2D6, as yet only eight have been subjected to experimental studies [36]. Therefore, involvement of other residues in binding and metabolism of CYP2D6-substrates remain to be established. For E216 and D301, it has been shown that they are important for the fixation of the basic nitrogen atom in ligands [13–15]. The strongly substrate dependent effects observed after mutagenesis of the aromatic residues F120 and F483 can be attributed either to the change in the active site topology upon removal of the phenylalanines, or can be due to loss of aromatic interaction points. The fact that the K_d values of wild-type CYP2D6 and CYP2D6[F483A] were very similar for the substrates tested suggests that the role of F483 in binding and metabolism of these compounds is mainly by influencing the statistics of possible orientations. However, advanced molecular modeling techniques such as molecular dynamics simulations can give further insight in these mechanisms.

Acknowledgement

We thank Mr. Ed Groot for his help with the expression and purification of CYP2D6 and CYP2D6[F483A].

References

[1] Evans WE, Relling MV. Pharmacogenomics: translating functional genomics into rational therapeutics. Science 1999;286:487–91.
[2] Mansuy D. The great diversity of reactions catalyzed by cytochromes P450. Comp Biochem Physiol C Pharmacol Toxicol Endocrinol 1998;121:5–14.
[3] Goeptar AR, Scheerens H, Vermeulen NPE. Oxygen and xenobiotic reductase activities of cytochrome P450. Crit Rev Toxicol 1995;25:25–65.
[4] Zanger UM, Raimundo S, Eichelbaum M. Cytochrome P450 2D6: overview and update on pharmacology, genetics, biochemistry. Naunyn Schmiedebergs Arch Pharmacol 2004;369:23–37.
[5] Anzenbacher P, Anzenbacherova E. Cytochromes P450 and metabolism of xenobiotics. Cell Mol Life Sci 2001;58:737–47.
[6] Ingelman-Sundberg M. Pharmacogenetics of cytochrome P450 and its applications in drug therapy: the past, present and future. Trends Pharmacol Sci 2004;25:193–200.
[7] Oscarson M. Pharmacogenetics of drug metabolising enzymes: importance for personalised medicine. Clin Chem Lab Med 2003;41: 573–80.
[8] Ingelman-Sundberg M, Oscarson M, McLellan RA. Polymorphic human cytochrome P450 enzymes: an opportunity for individualized drug treatment. Trends Pharmacol Sci 1999;20:342–9.
[9] Wormhoudt LW, Commandeur JNM, Vermeulen NPE. Genetic polymorphisms of human *N*-acetyltransferase, cytochrome P450, glutathione-S-transferase, and epoxide hydrolase enzymes: relevance to xenobiotic metabolism and toxicity. Crit Rev Toxicol 1999; 29:59–124.
[10] Ekins S, de Groot MJ, Jones JP. Pharmacophore and three-dimensional quantitative structure activity relationship methods for modeling cytochrome p450 active sites. Drug Metab Dispos 2001;29: 936–44.
[11] Vermeulen NPE. Prediction of drug metabolism: the case of cytochrome P450 2D6. Curr Top Med Chem 2003;3:1227–39.
[12] Koymans L, Vermeulen NPE, van Acker SA, te Koppele JM, Heykants JJ, Lavrijsen K, et al. A predictive model for substrates of cytochrome P450-debrisoquine (2D6). Chem Res Toxicol 1992;5:211–9.
[13] Ellis SW, Hayhurst GP, Smith G, Lightfoot T, Wong MM, Simula AP, et al. Evidence that aspartic acid 301 is a critical substrate-contact residue in the active site of cytochrome P450 2D6. J Biol Chem 1995;270:29055–8.
[14] Guengerich FP, Hanna IH, Martin MV, Gillam EM. Role of glutamic acid 216 in cytochrome P450 2D6 substrate binding and catalysis. Biochemistry 2003;42:1245–53.
[15] Paine MJ, McLaughlin LA, Flanagan JU, Kemp CA, Sutcliffe MJ, Roberts GC, et al. Residues glutamate 216 and aspartate 301 are key determinants of substrate specificity and product regioselectivity in cytochrome P450 2D6. J Biol Chem 2003;278:4021–7.
[16] Hayhurst GP, Harlow J, Chowdry J, Gross E, Hilton E, Lennard MS, et al. Influence of phenylalanine-481 substitutions on the catalytic activity of cytochrome P450 2D6. Biochem J 2001;355: 373–9.
[17] Keizers PH, Lussenburg BM, de Graaf C, Mentink LM, Vermeulen NPE, Commandeur JNM. Influence of phenylalanine 120 on cytochrome P450 2D6 catalytic selectivity and regiospecificity: crucial role in 7-methoxy-4-(aminomethyl)-coumarin metabolism. Biochem Pharmacol 2004;68:2263–71.
[18] Flanagan JU, Marechal JD, Ward R, Kemp CA, McLaughlin LA, Sutcliffe MJ, et al. Phe120 contributes to the regiospecificity of cytochrome P450 2D6: mutation leads to the formation of a novel dextromethorphan metabolite. Biochem J 2004;380:353–60.
[19] Ellis SW, Rowland K, Ackland MJ, Rekka E, Simula AP, Lennard MS, et al. Influence of amino acid residue 374 of cytochrome P-450 2D6 (CYP2D6) on the regio- and enantio-selective metabolism of metoprolol. Biochem J 1996;316(Pt 2):647–54.
[20] de Groot MJ, Ackland MJ, Horne VA, Alex AA, Jones BC. A novel approach to predicting P450 mediated drug metabolism. CYP2D6 catalyzed *N*-dealkylation reactions and qualitative metabolite predictions using a combined protein and pharmacophore model for CYP2D6. J Med Chem 1999;42:4062–70.
[21] Venhorst J, ter Laak AM, Commandeur JNM, Funae Y, Hiroi T, Vermeulen NPE. Homology modeling of rat and human cytochrome P450 2D (CYP2D) isoforms and computational rationalization of experimental ligand-binding specificities. J Med Chem 2003;46: 74–86.
[22] Kirton SB, Kemp CA, Tomkinson NP, St-Gallay S, Sutcliffe MJ. Impact of incorporating the 2C5 crystal structure into comparative models of cytochrome P450 2D6. Proteins 2002;49: 216–31.
[23] Smith G, Modi S, Pillai I, Lian LY, Sutcliffe MJ, Pritchard MP, et al. Determinants of the substrate specificity of human cytochrome P-450 CYP2D6: design and construction of a mutant with testosterone hydroxylase activity. Biochem J 1998;331:783–92.
[24] Kemp CA, Flanagan JU, van Eldik AJ, Marechal JD, Wolf CR, Roberts GC, et al. Validation of model of cytochrome P450 2D6: an in silico tool for predicting metabolism and inhibition. J Med Chem 2004;47:5340–6.
[25] Onderwater RC, Venhorst J, Commandeur JNM, Vermeulen NPE. Design, synthesis, and characterization of 7-methoxy-4-(aminomethyl)coumarin as a novel and selective cytochrome P450 2D6 substrate suitable for high-throughput screening. Chem Res Toxicol 1999;12:555–9.

[26] Braun U, Shulgin AT, Braun G. Centrally active N-substituted analogs of 3,4-methylenedioxyphenylisopropylamine (3,4-methylenedioxyamphetamine). J Pharm Sci 1980;69:192–5.
[27] Weinander R, Mosialou E, DeJong J, Tu CP, Dypbukt J, Bergman T, et al. Heterologous expression of rat liver microsomal glutathione transferase in simian COS cells and *Escherichia coli*. Biochem J 1995;311(Pt 3):861–6.
[28] Bauer S, Shiloach J. Maximal exponential growth rate and yield of *E. coli* obtainable in a bench-scale fermentor. Biotechnol Bioeng 1974;16:933–41.
[29] Omura T, Sato R. The carbon monoxide-binding pigment of liver microsomes. Ii. Solubilization, purification, and properties. J Biol Chem 1964;239:2379–85.
[30] Kranendonk M, Fisher CW, Roda R, Carreira F, Theisen P, Laires A, et al. *Escherichia coli* MTC, a NADPH cytochrome P450 reductase competent mutagenicity tester strain for the expression of human cytochrome P450: comparison of three types of expression systems. Mutat Res 1999;439:287–300.
[31] Yamazaki H, Nakamura M, Komatsu T, Ohyama K, Hatanaka N, Asahi S, et al. Roles of NADPH-P450 reductase and apo- and holo-cytochrome b5 on xenobiotic oxidations catalyzed by 12 recombinant human cytochrome P450s expressed in membranes of *Escherichia coli*. Protein Expr Purif 2002;24:329–37.
[32] Venhorst J, Onderwater RC, Meerman JH, Vermeulen NPE, Commandeur JNM. Evaluation of a novel high-throughput assay for cytochrome P450 2D6 using 7-methoxy-4-(aminomethyl)-coumarin. Eur J Pharm Sci 2000;12:151–8.
[33] Hanna IH, Krauser JA, Cai H, Kim MS, Guengerich FP. Diversity in mechanisms of substrate oxidation by cytochrome P450 2D6. Lack of an allosteric role of NADPH-cytochrome P450 reductase in catalytic regioselectivity. J Biol Chem 2001;276:39553–61.
[34] Lin LY, Di Stefano EW, Schmitz DA, Hsu L, Ellis SW, Lennard MS, et al. Oxidation of methamphetamine and methylenedioxymethamphetamine by CYP2D6. Drug Metab Dispos 1997;25:1059–64.
[35] Guengerich FP, Miller GP, Hanna IH, Sato H, Martin MV. Oxidation of methoxyphenethylamines by cytochrome P450 2D6. Analysis of rate-limiting steps. J Biol Chem 2002;277:33711–9.
[36] Guengerich F. Human cytochrome P450 enzymes. In: Montellano POd, editor. Cytochrome P450: structure, mechanism, and biochemistry. New York: Kluwer Academic/Plenum Publishers; 2005. p. 417.